DISCUSSION PAPER SERIES

DP15107

CAVEATS FOR ECONOMISTS: EPIDEMIOLOGY-BASED MODELLING OF COVID19 AND MODEL MISSPECIFICATIONS

Yinon Bar-On, Tatiana Baron, Ofer Cornfeld, Ron Milo and Eran Yashiv

MONETARY ECONOMICS AND FLUCTUATIONS

ISSN 0265-8003

CAVEATS FOR ECONOMISTS: EPIDEMIOLOGY-BASED MODELLING OF COVID19 AND MODEL MISSPECIFICATIONS

Yinon Bar-On, Tatiana Baron, Ofer Cornfeld, Ron Milo and Eran Yashiv

Discussion Paper DP15107
Published 29 July 2020
Submitted 28 July 2020

Centre for Economic Policy Research
33 Great Sutton Street, London EC1V 0DX, UK
Tel: +44 (0)20 7183 8801
www.cepr.org

This Discussion Paper is issued under the auspices of the Centre's research programmes:

- Monetary Economics and Fluctuations

Any opinions expressed here are those of the author(s) and not those of the Centre for Economic Policy Research. Research disseminated by CEPR may include views on policy, but the Centre itself takes no institutional policy positions.

The Centre for Economic Policy Research was established in 1983 as an educational charity, to promote independent analysis and public discussion of open economies and the relations among them. It is pluralist and non-partisan, bringing economic research to bear on the analysis of medium- and long-run policy questions.

These Discussion Papers often represent preliminary or incomplete work, circulated to encourage discussion and comment. Citation and use of such a paper should take account of its provisional character.

Copyright: Yinon Bar-On, Tatiana Baron, Ofer Cornfeld, Ron Milo and Eran Yashiv

CAVEATS FOR ECONOMISTS: EPIDEMIOLOGY-BASED MODELLING OF COVID19 AND MODEL MISSPECIFICATIONS

Abstract

Rapidly expanding research on COVID19 in Economics typically posits an economy subject to a model of epidemiological dynamics, which is at the core of the analysis. We place this model on the foundations of an epidemiological analysis of the SARS-CoV-2 virus transmission timescales. The contribution is twofold. First, we formulate a full model with epidemiologically-based and clinically-based parameterization. The model features two blocks: an infection transmission block, described by the SEIR-Erlang model, and a clinical block, characterizing the development of symptoms, hospitalization, ICU admission, and recovery or death. The latter is important for the analysis of dynamics of the public health system. Second, we show that there is often serious mis-specification of the model, erroneously characterizing a relatively slow-moving disease, thereby distorting the policymaker decisions towards less severe, delayed intervention. Moreover, the scale of the disease is under-estimated. We also discuss misguided modelling of lockdown policies.

JEL Classification: H12, I12, I18, J17

Keywords: the economy and epidemiological dynamics, COVID19, transmission timescales, optimal policy

Yinon Bar-On - yinon.baron@gmail.com
Weizmann Institute of Science

Tatiana Baron - tatian.baron@gmail.com
Ben Gurion University of the Negev

Ofer Cornfeld - ofer@cornfeld.co.il
BFI, Israel

Ron Milo - ron.milo@weizmann.ac.il
Weizmann Institute of Science

Eran Yashiv - yashiv@post.tau.ac.il
Tel Aviv University and CEPR

Acknowledgements
We thank seminar participants at UCL and LSE for comments. Any errors are our own.

Caveats for Economists: Epidemiology-Based Modelling of COVID 19 and Model Misspecifications*

Yinon Bar-On, Weizmann Institute of Science †

Tatiana Baron, Ben Gurion University ‡ **Ofer Cornfeld, BFI§**
Ron Milo, Weizmann Institute of Science‡

Eran Yashiv, Tel Aviv University, CfM (London School of Economics), and CEPR ¶

July 29, 2020

Abstract

Rapidly expanding research on COVID19 in Economics typically posits an economy subject to a model of epidemiological dynamics, which is at the core of the analysis. We place this model on the foundations of an epidemiological analysis of the SARS-CoV-2 virus transmission timescales.

The contribution is twofold. First, we formulate a full model with epidemiologically-based and clinically-based parameterization. The model features two blocks: an infection transmission block, described by the SEIR-Erlang model, and a clinical block, characterizing the development of symptoms, hospitalization, ICU admission, and recovery or death. The latter is important for the analysis of dynamics of the public health system.

Second, we show that there is often serious mis-specification of the model, erroneously characterizing a relatively slow-moving disease, thereby distorting the policymaker decisions towards less severe, delayed intervention. Moreover, the scale of the disease is under-estimated. We also discuss misguided modelling of lockdown policies.

*We thank seminar participants at UCL and LSE for comments. Any errors are our own.

†Department of Plant and Environmental Sciences, Weizmann Institute of Science, Rehovot, Israel.

‡Department of Economics, Ben Gurion University, Beer Sheva, Israel.

§BFI, Tel Aviv, Israel.

¶*Corresponding author.* The Eitan Berglas School of Economics, Tel Aviv University, Tel Aviv, Israel. and CfM, London School of Economics, London, UK. E-mail: yashiv@tauex.tau.ac.il; e.yashiv@lse.ac.uk

Key words: the economy and epidemiological dynamics, COVID19, transmission timescales, optimal policy, public health, disease dynamics and scale, clinical modelling, misspecification.

JEL No. H12,I12,I18, J17.

Caveats for Economists:
Epidemiology-Based Modelling of COVID 19 and Model Misspecifications

1 Introduction

Since March 2020 there has been a rapidly expanding research effort dedicated to COVID19 analysis across disciplines, inter alia, in Economics. A typical analysis posits an economy, which is subject to a model of epidemiological dynamics describing COVID19 disease dynamics. One type of economic analysis describes a planner problem that seeks to derive optimal policy. This trades off the costs of public health outcomes, such as breach of ICU capacity and death, with the economic costs of suppression policy, including declines in production, consumption, and investment. It leads to the modelling of the well-known concept of "flattening the curve" policy. Another strand of papers models the decentralized economy and the optimal decisions of agents, emphasizing individual epidemic-related behavior as well as externalities. In both cases the dynamics of the disease, as well as its features, like the fatality rate, are at the core of the analysis.

This paper makes two contributions: one is to place this analysis on the foundations of an epidemiological analysis of the SARS-CoV-2 virus properties. In particular, the timescales of disease transmission are examined. The main elements of the ensuing model are two blocks: an infection transmission block, where the number of new cases is determined, and is described by the SEIR-Erlang model; and a clinical block, which characterizes the development of symptoms, hospitalization, ICU admission and recovery or death. The former block derives from the epidemiologically-grounded analysis and defines epidemiological dynamics; the latter block is important in order to deal with the dynamics in the public health system. It offers a complete model of these two different dynamics, including epidemiologically-based and clinically-based parameterizations.

The second contribution is to show that there is often serious misspecification of the model, due to errors in the set-up and in the parameterization, at odds with the epidemiological evidence. These errors have important consequences for optimal economic planning and for policymaking relating to COVID19. In particular, they are manifested in erroneously characterizing a relatively slow-moving disease, thereby distorting the policymaker decisions towards less severe, delayed intervention, such as delayed lockdown. Moreover, the scale of the disease is under-estimated. The underlying cause for the misspecification is the failure to make the distinction between the epidemiological and clinical blocks. Wrong values are assigned to key parameters of disease dynamics, while other important parameters are omitted.

Finally, we revisit some prevalent approaches to modelling lockdown policies, highlighting problems in their main assumptions, and propose alternatives. In particular, the quadratic matching properties, flagged by economists, holds true only in highly unrealistic and implausible lockdown situations.

The analysis points economic researchers at the correct way to model the dynamics of the disease. This could serve well both types of analysis which were mentioned above. The analysis may also be useful for other epidemics beyond COVID19, as much of the discussion is pertinent to other forms of infectious diseases. Note, in this context, that the set of epidemics since 1980 is quite large and includes, inter alia, HIV/AIDS, SARS, H5N1, Ebola, H7N9, H1N1, Dengue fever, and Zika. We see the analysis here as complementary to the work of Ellison (2020), who focuses on the importance of the correct modelling of population heterogeneity in the context of COVID19.

The paper proceeds as follows: Section 2 presents key papers in the Economics literature which are relevant for the current discussion. Section 3 presents the epidemiological analysis of the SARS-CoV-2 virus transmission timescales. Section 4 discusses the epidemiological model which ensues from the latter analysis, and the parameterization that is appropriate to use. Section 5 presents the misspecified model used in part of the Economics literature, its parameterization, and its relation to the epidemiology-based model. Section 6 discusses the repercussions of using the wrong model. Section 7 briefly discusses the modelling of lockdowns. Section 8 concludes.

2 Literature

There has been an explosion of research in Economics on COVID19. Avery et al (2020) provide an early review and Baqaee, Farhi, Mina, and Stock (2020) offer a more recent discussion. Two kinds of papers have been making use of epidemiological models in ways that are relevant for the current analysis.

One is work using the concept of an optimizing planner. The point here is to examine in economic terms the losses due to the pandemic (e.g. deaths, breach of ICU constraints) and the economic consequences of public health policy (such as disease suppression measures, prominently lockdowns). In this framework an objective function is defined, with values taking into account economic losses and the value of statistical life. Thus, tradeoffs are measured and alternative policies can be evaluated. The planner constraints include, inter alia, the disease dynamics typically examined within the SIR epidemiological model. Prominent contributions include Acemoglu, Chernozhukov, Werning, and Whinston (2020), Akbarpour et

al (2020), Alvarez, Argente, and Lippi (2020), Chari, Kirpalani, and Phelan (2020), Farboodi, Jarosch, and Shimer (2020), and Jones, Philippon, and Venkateswaran (2020).

The second kind of work includes papers which tie macroeconomic dynamics to the epidemiological dynamics of the SIR model. These models posit that economic behavior has two-way connections with disease transmission. Notable contributions include Eichenbaum, Rebelo, and Trabandt (2020), and Krueger, Uhlig, and Xie (2020). Within the latter strand, the sectorial model of Kaplan, Moll, and Violante (2020) is notable for its careful analysis.

Depending on the exact formulation, we show below how erroneous use – which has been the case in some, but not all of the papers – might lead to work with misspecified models. This has substantial consequences for policy. Two key properties of disease dynamics, its scale and speed, are at the center of misspecification.

3 Epidemiological Analysis of the SARS-CoV-2 Virus Transmission Timescales

At the core of many mathematical frameworks for modeling the spread of infectious diseases such as COVID19, lie key timescales which characterize the transmission of the disease between individuals, as well as its progression within an infected individual. These concepts lie at the foundation of the renewal equation approach, advanced by Lotka (1907), and the compartmental model approach, proposed by Kermack and McKendrick (1927). In what follows we present these approaches briefly. For a description of the evolution of the literature and a mathematical treatment of the equivalence of the two approaches, see Champredon, Dushoff, and Earn (2018).

3.1 The Generation Interval and the Renewal Equation

The most basic relevant timescale used in this context is known as the generation interval, which is defined for an infector-infectee pair. The generation interval is the time between the infection of the infector and the infection of the infectee. This duration of the generation interval is hard to quantify directly, as it is hard to pinpoint the exact time in which transmission occurred. The more commonly observed quantity is known as the serial interval, which measures the time between symptom onset in the infector and symptom onset in the infectee. To infer the generation interval from the observed serial interval, a third timescale is needed. This timescale, known as the incubation period, is defined as the time from infection with the virus

until symptom onset. It is clear that these three timescales could vary significantly between individuals, and thus they are better represented at the population level as probability density functions. References to key studies and details on these timescales are provided in Bar-On, Sender, Flamholz, Phillips, and Milo (2020).

Once the distribution of generation intervals is inferred, it can be used in the context of a common mathematical framework for modeling the disease – the so called Lotka-Euler renewal equation.[1] In its simplest form, the renewal equation posits that:

$$I(t) = \int_0^\infty I(t-\tau) \cdot \beta(\tau) d\tau \tag{1}$$

where $I(t)$ is the number of infected people at time t, and $\beta(\tau)$ is the transmission rate of people in day τ after their infection (in units of days^{-1}). The function $\beta(\tau)$ is also known as the infectiousness profile, and is defined to be the same as the probability distribution function of the generation interval, scaled by the basic reproduction number $\mathcal{R}_0$, which is the average number of people an infected person infects over the course of their infection:

$$\beta(\tau) = \mathcal{R}_0 \cdot g(\tau) \tag{2}$$

where $g(\tau)$ is the generation interval distribution.

3.2 The Compartmental Approach

An equivalent modeling approach attempts to discretize the infectiousness profile by splitting up the infectiousness profile of an infected individual into distinct compartments – the Exposed (E), Infectious (I), and Resolved (R) compartments. This discretization is at the heart of the Susceptible-Exposed-Infectious-Resolved ($SEIR$) model. In both the E and R compartments, infectiousness is zero, whereas in the I compartment, the transmission rate is β. An infected individual spends a certain amount of time in each compartment, before moving to the next compartment. The time spent in the E and I compartments are known as the latent[2] and infectious periods, respectively. The overall infectiousness across the entire disease progression for an infected individual, which is the reproduction number $\mathcal{R}_0$, is a constant β times the infectious period. The $SEIR$ model can be defined in terms of differential equations in the following manner:

[1] The renewal equation was introduced by Leonhard Euler in 1767 in work on population dynamics. It was reformulated in a more general continuous version by Alfred Lotka, father of the field of mathematical demography (see Lotka (1907)).

[2] Not to be confused with the incubation period, which is the time it takes from infection to symptoms appearance.

$$\dot{S}(t) = -\beta \cdot I(t) \cdot S(t) \quad (3)$$

$$\dot{E}(t) = \beta \cdot I(t) \cdot S(t) - \sigma E(t) \quad (4)$$

$$\dot{I}(t) = \sigma E(t) - \gamma I(t) \quad (5)$$

$$\dot{R}(t) = \gamma I(t) \quad (6)$$

where S, E, I and R are the fractions of the population in the respective compartments, β is the transmission rate during the infectious period,[3] σ is the rate at which a person moves from the E to the I compartment and γ is the rate at which a person moves from the I to the R compartment. Because σ and γ are constant, this implies that the time spent in either the E and I compartments is exponentially distributed with a mean of $1/\sigma$ and $1/\gamma$. As the time spent in the E and I compartments are the latent and infectious periods, this implies the shape of these periods is distributed according to the following formulae:

$$T_L(t) = \sigma \exp(-\sigma t);\ T_I(t) = \gamma \exp(-\gamma t) \quad (7)$$

where $T_L(t)$ and $T_I(t)$ are the probability density functions of the latent and infectious periods, respectively.

Exponentially distributed latent and infectious periods imply that most people spend zero amount of time being either in their latent period or in their infectious period, which is not accurate biologically. Therefore, to produce more accurate distributions for the exposed and infectious periods, with a mode near the mean, one models the E and I compartments as split into two (or more) each, with double the rate of transfer between them. We present the ensuing differential equations in the next section. Now, the latent and infectious periods are the sum of the time spent in the E_1 and E_2 or I_1 and I_2 sub-compartments, respectively, and their distribution is thus the same as that of a sum of exponentially distributed random variables. The distribution of the sum of m exponentially distributed random variables is known as the Erlang distribution, which is a special case of the Gamma distribution with an integer as the shape parameter of the distribution. This type of augmented model is known as the SEIR-Erlang model, and the corresponding probability density distributions for the latent and infectious periods are now described by the following formulae:

$$T_L(t) = (2\sigma)^2 t \exp(-2\sigma t);\ T_I(t) = (2\gamma)^2 t \exp(-2\gamma t) \quad (8)$$

[3]To avoid clutter we leave out time indices for β and $\mathcal{R}$, since their time-variability is not at the focus of the paper and our results and intuition are invariant to the assumptions on $\mathcal{R}$ dynamics. However we do use a specification with a regime-dependent $\mathcal{R}$ when we discuss the optimal planner problem below.

The means of these distributions are still $1/\sigma$ and $1/\gamma$, but now the modes of the distribution are also near $1/\sigma$ and $1/\gamma$.

4 A Model Based on the Epidemiological Evidence

We analyze the evolution of the disease in two complementary blocks – infection transmission and clinical progression. The infection transmission block is the one where the number of new cases is determined, and is described by the SEIR-Erlang model. The clinical block characterizes the development of symptoms, hospitalization, ICU admission and recovery/death. The former block derives from the afore-going epidemiological-grounded analysis and defines the epidemiological dynamics; the latter block is important in order to deal with the dynamics in the public health system.

4.1 The SEIR-Erlang Block

Following the analysis of Karin et al (2020), we shall use the SEIR–Erlang model with two sub-compartments.[4] Graphically, this model is represented in panel a of Figure 1.

Figure 1

Analytically the following equations describe this block. Throughout, all stock variables are expressed as a fraction of the population.

$$\dot{S}(t) = -\beta \cdot (I_1(t) + I_2(t)) \cdot S(t) \tag{9}$$

$$\dot{E_1}(t) = \beta \cdot (I_1(t) + I_2(t)) \cdot S(t) - 2\sigma E_1(t) \tag{10}$$

$$\dot{E_2}(t) = 2\sigma E_1(t) - 2\sigma E_2(t) \tag{11}$$

$$\dot{I_1}(t) = 2\sigma E_2(t) - 2\gamma I_1(t) \tag{12}$$

$$\dot{I_2}(t) = 2\gamma I_1(t) - 2\gamma I_2(t) \tag{13}$$

$$\dot{R}(t) = 2\gamma I_2(t) \tag{14}$$

[4]Karin et al (2020) simulated the cases of two sub-compratments and examined them relative to the cases of one, or more than two, sub-compartments, and found two sub-compartments to be a reasonable formulation.

4.2 The Clinical Block

The SEIR-Erlang block does not describe the clinical progression of the disease. Hence, it does not provide information on the timing and the shares of people developing symptoms, being hospitalized and admitted to ICU. The clinical block does that, describing how new cases progress through the public health system. Concurrently with the progression of an infected person through the infectiousness compartments described above, over the course of the disease the same person progresses through the public health system. This latter process depends on the development of symptoms and on the severity of those. In more serious cases a person gets hospitalized and in some cases has to be moved to an intensive care unit (ICU). It is very important to note that the onset of symptoms and the subsequent clinical developments follow a separate time-scale that is different from the latent and infectious periods described above. The same applies to the timing of transition into an ICU. Since the progression of an infected person through the public health system follows a separate track from one's progression through the infectiousness stages, in what follows we suggest to separate these two tracks in the model as well. Adequate modelling of the clinical progression is important for the derivation of optimal policy that takes into account the burden on the public health system.

We thus postulate the following. Once infected, a person enters a state P during which there are still no symptoms and it is not known whether the symptoms will eventually appear. This period – the incubation period – lasts for $1/\theta_P$ on average and at its end, a person either remains asymptomatic (O) or develops symptoms (M). Denote the share of cases that remain asymptomatic by η. Asymptomatic people do not crowd hospitals, they go to work, and at some point, recover. Symptomatic cases (share $1-\eta$ of cases) might develop serious symptoms and get hospitalized (H). This happens with probability ξ. Once in a hospital, a given share π of patients develop conditions requiring transition to ICU (denoted X). Once in ICU, a fraction $\delta(\cdot)$ dies. We specify the latter probability of death, once in ICU, as:

$$\delta(X(t), \overline{X}) = \delta_1 + \delta_2 \cdot \frac{\mathbf{I}(X(t) > \overline{X}) \cdot \left(X(t) - \overline{X}\right)}{X(t)} \tag{15}$$

where $\overline{X}$ denotes ICU capacity and $\mathbf{I}$ is the indicator function.

Finally, at any stage, a person may recover (C). The clinical block is represented graphically in panel b of Figure 1.

We now present the analytical description of the model. Note that we describe here only the evolution of the symptomatic branch of the scheme, and do not describe the evolution of the pool of the recovered (C). This is so because for the economic analysis, discussed below, one only needs to

predict the number of people who are not able to work, and the number of people who develop conditions requiring intensive care.[5]

$$\dot{P}(t) = \beta \cdot (I_1(t) + I_2(t)) \cdot S(t) - \theta_P \cdot P(t) \quad (16)$$

$$\dot{M}(t) = (1 - \eta) \cdot \theta_P \cdot P(t) - \theta_M \cdot M(t) \quad (17)$$

$$\dot{H}(t) = \xi \cdot \theta_M \cdot M(t) - \theta_H \cdot H(t) \quad (18)$$

$$\dot{X}(t) = \pi \cdot \theta_H \cdot H(t) - \theta_X \cdot X(t) \quad (19)$$

$$\dot{D}(t) = \delta(X(t)) \cdot \theta_X \cdot X(t) \quad (20)$$

The parameters θ_M, θ_H, and θ_X denote the average time that passes between symptoms onset and hospitalization, hospitalization and ICU admission, and ICU admission and death, respectively.

4.3 Connection to Economic Analysis

The connection to economic analysis can be made by positing that the number of people who can work daily $N(t)$ is given by:

$$N(t) = l \cdot \rho \cdot (1 - D(t) - X(t) - H(t) - \phi M(t)) \quad (21)$$

where $0 < l < 1$ is the employment fraction out of the total population (subject to standard labor supply arguments), $0 < \rho \leq 1$ is the fraction able to work given any policy restrictions during the pandemic, and $0 \leq \phi \leq 1$ is the fraction of people with symptoms who do not work. If $\phi = 1$, it means that anyone who develops symptoms self-isolates immediately and does not work.

4.4 Parameterization

It should be clear from the preceding discussion that the parameterization of this model needs to be epidemiologically-based and clinically-based. In Table 1 we present the relevant values for the two blocks, where we rely on the analysis in Bar-On, Sender, Flamholz, Phillips, and Milo (2020) and sources in the epidemiological and medical literatures, as elaborated in the table notes.

Table 1

[5]Note that in the equation for $\dot{P}(t)$, presented here, we use $-\dot{S}(t) - \theta_P \cdot P(t)$ on the RHS and insert $\dot{S}(t) = -\beta \cdot (I_1(t) + I_2(t)) \cdot S(t)$.

Two elements are noteworthy:

(i) The transmission rate $\beta = \gamma \cdot \mathcal{R}$ depends on the regime – in lockdown it is denoted $\gamma \cdot \mathcal{R}_L$, and out of lockdown (work) it is denoted $\gamma \cdot \mathcal{R}_W$.

(ii) The Infection Fatality Rate (IFR) is 0.8%,[6]consistent with the estimates of the Imperial College COVID-19 Response Team (2020).

Additionally, we parameterize the rate the probability δ as follows, noting that $\delta(X(t), \overline{X}) = \delta_1 + \delta_2 \cdot \frac{\mathbf{I}(X(t)>\overline{X}) \cdot \left(X(t)-\overline{X}\right)}{X(t)}$. Based on Bar-On, Sender, Flamholz, Phillips, and Milo (2020) we set $\delta_1 = 0.5$. In the U.S. economy, ICU capacity is $\overline{X} = \frac{58{,}094}{329.529 * 10^6} = 1.8 \times 10^{-4}$. This is based on an estimate of $58,094$ ICU beds by the Harvard Global Health Institute.[7] Finally, following Kaplan, Moll, and Violante (2020) we set $\delta_2 = 0.5$.

5 Alternative Specifications

The overwhelming majority of Economics papers on COVID19 model clinical outcomes and infections dynamics within a single block. In many cases the calibration of this single framework has been guided by two basic numbers that pertain to two conceptually different processes – the spread of the disease and its clinical progression:

a. The basic reproduction number $\mathcal{R}_0$. This is often calibrated at 2.50, following various sources, for example CDC estimates.[8]

b. Duration till death. It takes on average 18-19 days to die from COVID19, once one gets infected (Imperial College COVID-19 Response Team (2020)).

In subsection 5.1 we present an oft-used model together with its calibration, based on the targets above. In subsection 5.2 we present a modification of the latter model and its parameterization so that it becomes closer to the benchmark of the preceding section.

5.1 The Widely-Used SIR Model

Economists modelling the dynamics of COVID19 have mostly been using versions of a SIR model, which is a special case of the model discussed above and the problematics of which are going to be analyzed below. It has the following structure.

$$\dot{S}(t) = -\beta \cdot I(t) \cdot S(t) \tag{22}$$

$$\dot{I}(t) = \beta \cdot I(t) \cdot S(t) - \gamma I(t) \tag{23}$$

$$\dot{R}(t) = \gamma I(t) \tag{24}$$

[6]The IFR here is given by $(1-\eta) \cdot \xi \cdot \pi \cdot \delta_1 = 0.5 \cdot 0.08 \cdot 0.4 \cdot 0.5 = 0.008$

[7]See https://globalepidemics.org/our-data/hospital-capacity/

[8]https://www.cdc.gov/coronavirus/2019-ncov/hcp/planning-scenarios.html#table-1

Whenever numbers of deceased and recovered are needed the following equations are also used:

$$\dot{D}(t) = \eta \dot{R}(t) \tag{25}$$

$$\dot{C}(t) = (1-\eta)\dot{R}(t) \tag{26}$$

where D is deceased and C is recovered.

The resulting prevalent calibration is the following:

$$1/\gamma = 18 \Longrightarrow \gamma = 1/18$$

$$\beta = \mathcal{R}_0 \cdot \gamma = 2.50 \cdot 1/18 = 0.139$$

Thus:

a. The duration of the disease till death is exactly the duration of the Infected stage, and it is $1/\gamma$.

b. The infection transmission rate β is pinned down by the basic reproduction rate $\mathcal{R}_0$ and the parameter governing the length of the infectious stage. In this simple SIR model, the infectious period coincides with the infected stage I and is therefore defined by γ.

5.2 The SIRD Model

Note that the widely-used SIR model and its parameterization presented above imply that an infected person becomes infectious immediately upon catching the disease and remains infectious throughout the entire disease duration. Therefore, the framework contradicts the two following facts established in the epidemiological analysis of COVID19:

a. People who get infected are not immediately infectious as there is a latent period at the beginning of the disease. We have denoted this stage by E, standing for "exposed." The existing evidence, used in Table 1, is that this period lasts on average around 3 days.

b. People are infectious during a relatively short period of time. After one stops being infectious, the disease continues, and some time should pass till one recovers or dies,. During this time one does not transmit the disease anymore. The evidence (see Table 1) is that the period of infectiousness lasts only around 4 days on average.

These two facts are fully reflected in the SEIR model and its epidemiology-grounded parameterization, on which we have expounded in Section 4. However, it is possible to introduce a modification of the SIR model, which has also been sometimes used by economists, that makes it more relevant in light of the two points above. Thus we modify the SIR model above,

given by equations (22)-(24), so as to take into account the correct timing of the disease until resolution. Hence we replace equation (24) by:

$$\dot{R}(t) = \gamma I(t) - \theta \cdot R(t) \tag{27}$$

The parameter θ governs the duration of the resolving stage R. Note that now, replacing equations (25)-(26), one gets:

$$\dot{D}(t) = \eta \cdot \theta \cdot R(t) \tag{28}$$

$$\dot{C}(t) = (1-\eta) \cdot \theta \cdot R(t) \tag{29}$$

This model is often called the $SIRD$ model. Based on the afore-cited epidemiological properties and the same targets discussed for the SIR model, one may parameterize the $SIRD$ model as follows:

$$\gamma = 1/7$$

$$\theta = 1/11$$

$$\beta = \mathcal{R}_0 \cdot \gamma = 2.5 \cdot 1/7 = 0.357$$

5.3 Relations Between the Specifications

In what follows we shall consider four different model specifications:

a. models (i) + (ii) – the full $SEIR$-Erlang model, discussed above in Section 4; we look at our preferred specification of two compartments (model i, denoted SEIR-2, see sub-section 4.1) as well as at one compartment (model ii, denoted SEIR, see equations (3)-(6) in sub-section 3.2);

b. model (iii) – the simple, widely-used SIR model parameterization discussed in sub-section 5.1;

c. model (iv) – the $SIRD$ model of sub-section 5.2.

Note a number of notational differences across the specifications:

a. The overall scale of the epidemics is measured by I in SIR and $SIRD$, by $E + I$ in $SEIR$, and by $E_1 + E_2 + I_1 + I_2$ in $SEIR - 2$.

b. In the $SIRD$ model, the state R is interpreted as Resolving and has duration governed by θ. This is in contrast to the removed/resolved state R in the other models.

Figure 2 illustrates these different specifications and presents the values given to the key parameters.

Figure 2

The key difference between the models lies in the implied infection transmission rate β as seen in the fourth row of the table in Figure 2. The implied β follows immediately once the length of the infectious period $1/\gamma$ is set. The specifications that assume a long infectious period, for example the SIR model, have to posit a low transmission rate β in order to match a particular value of $\mathcal{R}_0$. The specifications that assume an epidemiologically-grounded short infectious period (for example, the $SEIR$ and $SEIR-2$, or, to a lesser extent, the $SIRD$ model), can only match $\mathcal{R}_0$ if the transmission rate per unit of time β is relatively high. The separation of the infections generation block from the clinical block lies at the heart of the differences between the widely-used SIR parameterization and the benchmark $SEIR-2$ model (see Section 4 above) or its simplified counterpart $SEIR$. Mixing the two distinct timescales in a one-block parameterization is behind the calibration of SIR, the problematics of which we discuss below. The modification of SIR, called $SIRD$, presented in sub-section 5.2, makes this problem somewhat less acute by adding a parameter θ that governs the duration of the resolving stage, while still targeting $\mathcal{R}_0$ and duration-till-death in a single block. In the next section, we consider the implications of these misspecifications for disease dynamics, the burden on the public health system, and planner optimization.

6 The Implications of Misspecification

We turn now to explore the implications of the different dynamics inherent in the models shown in Figure 2. To do so we start with an exploration of the speed of the disease across models (sub-section 6.1), then study the dynamics in terms of the reproductive number, $\mathcal{R}$ (in 6.2), and end by discussing the implications for optimal policy (6.3).

6.1 The Speed of the Disease

The length of the infectious period, governed by γ, has important effects on the implied epidemic dynamics. At the start of the epidemic $S(0) \simeq 1$, so the SIR model of sub-section 5.1 has the following approximate solution for I using the dynamic equation (23):

$$I(t) = I(0)\, e^{\lambda t} \tag{30}$$

where $\lambda = \gamma(\mathcal{R}_0 - 1)$.

As seen in Figure 2, the different models imply very different growth rates of the disease. In particular, while all models, except for the widely-used SIR imply disease daily growth rates of $17\% - 21\%$, the SIR model itself implies 8%; the disease doubles in $3.2 - 4.2$ days under the three models but takes 8.3 days to double in the widely-used SIR model. This is a

first-order effect, with the mis-calibrated SIR model implying much slower disease dynamics.

More generally, panels a and b in Figure 3 illustrate the development of the disease, as measured by the stock of infectious and exposed people[9] (panel a) and hospitalized in ICU (panel b), under the different models depicted in Figure 2.

Figure 3

The length of the infectious period, governed by γ, has important effects on the implied epidemic dynamics.

a. *Slow disease in the widely-used SIR.* From Figure 3 and Table 1 one sees that a specification with a very long infectious period – the SIR model with $\gamma = 1/18$ – implies a much lower transmission rate β and therefore the disease progresses much more slowly; the epidemic is spread out in time, and the maximal number of infected at a given point in time reaches 24% of the population on day 120. It takes almost 330 days for the epidemic to die out.

b. *Faster dynamics in SEIR and SIRD.* By contrast, specifications with a relatively short infectious period, the $SEIR$ models and the $SIRD$ model, imply much faster dynamics. The epidemic starts aggressively and cases rise very fast, reaching the peak on days 59 (for $SEIR$), 56 (for $SEIR-2$), and 49 (for $SIRD$). The epidemic also dies off quickly; there are hardly any people in I after day 120, and the entire episode ends twice as fast as under the SIR model calibration.

Note that these numbers pertain to an unmitigated disease and thus do not correspond to real world data.

c. *Effects on ICU utilization.* Panel b of Figure 3 shows that with a slow moving disease, implied by a long infectious period, ICU capacity is breached on day 82, and peak demand exceeds capacity by a factor of 7, whereas in the epidemiological-grounded model it is breached much earlier, on day 41, and peak demand exceeds capacity by a factor of 14.

d. *Role of the latent period.* Ignoring the short latent period (E), as in SIR and $SIRD$, has moderate effects on epidemic dynamics. In $SIRD$, relative to the two SEIR models, the epidemic develops a bit faster at the beginning, because there is no delay between the moment a person becomes infected and the moment he or she starts spreading the disease.

e. *The role of sub-compartments.* Dividing I and E into sub-compartments and the number of sub-compartments have some effects on both the speed and the scale of the disease. Using only one compartment for I and E implies a model of the dynamics such that most of the people exposed become infectious immediately and most of the infected recover immediately. This is counter-factual. When the economy is in the phase of a rising disease,

[9] In the case of SIR – infectious only.

each compartment and sub-compartment is more populated that the compartment following it. Every day there are more people who are exposed than there are people who are infectious, and more people are infected today than yesterday, in line with exponential growth.

From Figure 3 one can see that with different numbers of sub-compartments, disease dynamics change. The underlying dynamics (not shown) are that in the $SEIR$ model, the disease slows down with the number of E sub-compartments and rises faster in the number of I sub-compartments; when both E and I sub-compartments are increased, the combined effect depends on model parameters. Specifically, in COVID19 where $\gamma < \sigma$, the disease speed is faster when increasing the number of both sub-compartments in E and I.

Moreover, in the $SEIR-2$ model with two sub-compartments, more people are infected before the entire population reaches herd immunity, and a higher level of disease is reached. At the peak, the number of infectious/exposed people reaches 27% of the population (a difference of 3.5% relative to the other models, or 11.6 million people in the case of the U.S). This can be seen in the higher peak of the red lines in I and in X in Figure 3 and in the numbers presented in panel c of Table 2.

f. *Implications for initial conditions.* Under equal initial conditions, it takes much more time for the epidemic to gain pace under the widely-used SIR model than under SEIR. One can try to 'circumvent' this problem by assuming a higher initial seed of the infection. Panel c of Figure 3 compares the SEIR model with initial seed of 10^{-4} and the widely-used SIR model with initial seed of 10^{-2}. It shows that assuming a higher initial seed does place SIR on the same timescale as SEIR in terms of the length of the entire episode and timing of the peak. However, two problems remain.

First, at peak, the implied number of infectious individuals is still way lower under SIR, which distorts the problem of a policymaker constrained by a number of hospital/ICU beds.

Second, assuming a seed of 1% of the population implies, in terms of the U.S. economy, that the epidemic has started when over 3.3 million people got infected. This is a highly implausible assumption, given the actual data on the time path of known cases and on deaths.

These properties, relating to the speed and scale of the disease, are crucial in any framework where a planner or a policymaker wants to manage the disease optimally, and faces an ICU capacity constraint. We illustrate this in sub-section 6.3 below.

6.2 Initial Disease Dynamics and the Reproduction Number

As mentioned, the Lotka–Euler equation is a basic equation in demography, used for the study of age-structured population growth. It is similarly used in epidemiology to study disease growth. One possibility is to retrieve the

reproduction number, $\mathcal{R}_0$, from the growth rates of the disease. Following Wallinga and Lipsitch (2007), the characteristic equation of Lotka-Euler is given by:

$$1 = \int_0^\infty e^{-\lambda\tau} \cdot \beta(\tau) d\tau \tag{31}$$

Using equations (1), (2), and (31) they get:

$$\frac{1}{\mathcal{R}_0} = \int_0^\infty e^{-\lambda\tau} g(\tau) d\tau \tag{32}$$

The term on the right-hand side of equation (32) is the Laplace transform of the function $g(\tau)$. It is also the moment generating function $M(\lambda)$ of the distribution $g(\tau)$.

Thus:

$$M(\lambda) = \int_0^\infty e^{\lambda\tau} g(\tau) d\tau \tag{33}$$

and so:

$$\mathcal{R}_0 = \frac{1}{M(-\lambda)} \tag{34}$$

Wallinga and Lipsitch (2007) go on to show the explicit expression for $\mathcal{R}_0$ using different formulations of $g(\tau)$ and hence $M(\lambda)$.

For the case of the SIR model ($\sigma = 0$) this is given by:

$$\mathcal{R}_0 = 1 + \frac{\lambda}{\gamma} \tag{35}$$

In the SEIR model with one compartment it is given by:

$$\mathcal{R}_0 = \left(1 + \frac{\lambda}{\gamma}\right)\left(1 + \frac{\lambda}{\sigma}\right) \tag{36}$$

In the compartmental SEIR model with m, n compartments it is given by (using equation 4 in Wearing et al (2005)):[10]

$$\mathcal{R}_0 = \frac{\lambda\left(\frac{\lambda}{\sigma m}+1\right)^m}{\gamma\left(1 - \left(\frac{\lambda}{\gamma n}+1\right)^{-n}\right)} \tag{37}$$

The above formulae (35)-(37) are presented in Figure 2; once the value of λ is known, the figure provides numerical values for all other parameters needed to compute $\mathcal{R}_0$.

[10]The original publication of Wearing et al (2005) contained an error. This equation is the corrected version; see 2005 Correction: Appropriate models for the management of infectious diseases. **PLoS Med 2(8)**: e320.

We can now see that incorrect parameterization of the length of the infectious period $1/\gamma$, as shown in Figure 2 for the case of SIR model, distorts the true properties of disease dynamics. Suppose, for example, that one were to use the expression (35) above to recover the basic reproduction number $\mathcal{R}_0$, rather than just taking it to be of a particular value. The transmission rate β would then be:

$$\beta = \mathcal{R}_0 \cdot \gamma = \gamma + \lambda \tag{38}$$

Equation (38) shows that even when we do not fix $\mathcal{R}_0$ in advance, but recover it from the data on the infections growth rate λ, assuming, erroneously, a low γ will result in a low transmission rate β, implying much less aggressive epidemics dynamics.

6.3 Implications for an Optimizing Planner Problem

To illustrate the consequences of the wrong parameterization of γ for the outcomes, in particular for the number of deaths and breach of ICUs, we use an optimizing planner model developed in Alon et al (2020). The planner minimizes the following loss function:

$$\min \int_{t=0}^{\infty} e^{-rt} \left(\frac{Y(t)}{N(t)} \left(N^{ss} - N(t) \right) + \chi \dot{D}(t) \right) dt \tag{39}$$

The loss function is minimized in PDV terms (r is the discount rate) over infinite horizon, where at finite point T_V (set at 540 days) the vaccine is found and the pool of susceptibles drops to zero, so that the disease stops growing. It includes lost output $(\frac{Y(t)}{N(t)}(N^{ss} - N(t))$, the average output per worker multiplied by the decline in employment relative to steady state) and the value of lost life $(\chi \dot{D}(t))$. The latter argument is affected, inter alia, by the breach of ICU (which affects $\dot{D}(t)$) as modelled in equation (15) above. The planner thus faces the tradeoff whereby a prolonged lockdown leads to economic costs, while a breach of ICU, as lockdowns are stopped, leads to increased costs of life. Note two elements that affect these dynamics – "herd immunity," where the disease reaches a point in time from which it declines ($\dot{I}(t) < 0$), and the arrival of a vaccine (T_V).

To work within a realistic set-up, we let the planner decide on when to start and when to stop lockdown. In Alon et al (2020) we allow for alternative lockdown strategies and for more choices of timing. Here we simplify and allow one choice, of the start and end of a full lockdown (allowing, though, for essential workers and remote work, throughout). We use the parameter values of Figure 3 and the following time path for $\mathcal{R}$. We start off from a value of 2.50 consistent with the findings of Jones and Villaverde

(2020) inferring $\mathcal{R}_0$ from empirical data. Subsequently, following the review of the literature in Karin et al (2020) and their estimates of $\mathcal{R}$ in work and lockdown periods, we use $\mathcal{R}_W = 1.50$ for work periods that follow a lockdown period and $\mathcal{R}_L = 0.80$ for the lockdown period itself. Referring to the U.S. economy, we use $\rho = 0.7$ for the value of the fraction able to work in a lockdown, following evidence cited in Alon et al (2020), and $\chi = 85.7$ for the value of lost life following Hall, Jones, and Klenow (2020) and Greenstone and Nigam (2020).[11]

We undertake the following exercise. We take this planner problem, and solve it for the optimal timing of lockdown (the start and end dates) under the afore-cited SIR model plugged into the infection transmission block. This features the implausibly low value of $\gamma = 1/18$. We subsequently compare deaths and the share of people in ICU across the following two scenarios: (i) the planner implements the policy above and the true model is indeed SIR with $\gamma = 1/18$, in accordance with what was assumed when devising the policy (to be denoted 'planned' in the figure below), and (ii) the planner implements the same policy but the true model is $SEIR-2$ with $\sigma = 1/3$, $\gamma = 1/4$ (denoted 'realized' in the figure below). Comparing these two scenarios gives a sense of the cost of the errors made when using the wrong model and parameter values. Figure 4 illustrates, with the shaded areas denoting the period of lockdown chosen by the planner who is using SIR with $\gamma = 1/18$.

Figure 4

In the first scenario, where the planner is correct in the perception of disease dynamics, lockdown begins on day 75 (start of the shaded area). Following the blue lines, one can see that the economy then experiences a small breach of ICU capacity; in panel b of Figure 4, X attains $2.4 * 10^{-4}$ while $\overline{X} = 1.8 * 10^{-4}$. This is followed by a decline in infections, as seen in panels a and b. After lockdown is released, on day 147 (end of the shaded area) there is a smaller second wave of the disease, which does not breach ICU capacity. The disease declines to below 0.5% on day 454 and the cumulative death rate is 0.43%. In U.S. terms this is 1.43 million people. The

[11] We follow the analysis in Hall, Jones, and Klenow (2020), who state that estimates of the Value of Statistical Life per year in the U.S. range from \$100,000 to \$400,000, and that COVID deceased have an expected average of 14 years of life remaining. Taking the upper end figure, following Greenstone and Nigam (2020), and U.S. GDP per capita at \$65,351 this yields:

$$\begin{aligned} \chi &= \frac{\text{expected years remaining} \cdot VSLY}{\frac{Y}{POP}} \\ &= \frac{14 * 400,000}{65,351} = 85.7 \end{aligned}$$

attained values of the loss function (loss of annual GDP in PDV terms) is 0.42 in total loss, out of which 0.06 is loss of output, and 0.36 is loss of life.

What is the planner doing? Using lockdown to suppress the disease for 540 days (until the vaccine is found) is not a viable option as it is too expensive. Therefore the planner tries to minimize death under these circumstances. The two ways to minimize death are to avoid breaching the ICU limit and to avoid overshooting the herd immunity threshold (which, for $\mathcal{R}_W = 1.50$, is at $S^* = 0.67$). The planner's choice is to time the lockdown so as to get two waves. The first one breaches the ICU limit only slightly (death of 75 people per million); the second one does not breach the ICU limit. However, there is still significant overshooting of the herd immunity threshold, by 18 percentage points, with $S(T_V) = 0.48$ vs. $S^* = 0.67$. The planner prefers the latter over breaching the ICU limit that might double the death rate.

In the second scenario, the planner is mistaking the speed of the disease and thus the severity of the situation. The disease is much faster than planned, and most of the outbreak happens before the lockdown is imposed. The reproduction parameter $\mathcal{R}$ is reduced to 1.50 when the peak has already passed, rendering the lockdown timing even more irrelevant. The epidemics rages basically unmitigated and declines to below 0.5% on day 81. Eventually the overshooting of the herd immunity threshold is huge, with $S(T_V) = 0.11$ rather than $S^* = 0.67$. Following the red lines, one can see that there is an enormous breach of ICU capacity; X attains $24 * 10^{-4}$ i.e., ten times as much as expected by the planner (recall that $\overline{X} = 1.8 * 10^{-4}$). The number of deaths increases to $D = 12,962$ per million, out of which $5,859$ per million are due to the breaching of ICU capacity, and the cumulative death rate is 1.29%, which in U.S. terms is 4.28 million people. Loss of annual GDP in PDV terms is 1.18 for total loss, out of which 0.08 is loss of output, and 1.1 is loss of life (GDP per annum, in PDV terms). There is a tremendous cost in terms of loss of life generated by misperception of the dynamics of the disease.

Three remarks are in place as to the numbers of deceased in this analysis. One is that in Alon et al (2020) we show that much more favorable outcomes, with much lower death numbers, can be attained when allowing the planner more choices of lockdown strategies. The cost of mis-specification, though, remains high. The second, and related to the first, is that in the real world, U.S. death numbers are currently almost $150,000$, or 0.04% , an order of magnitude lower than even the relatively 'benign' first scenario above. This is so because U.S. policymakers have imposed longer lockdowns than the planner above, as they have access to wider policy choices. Third, most papers, which model the SIR-based planner, actually present even higher numbers of deaths, in the order of magnitude of the second scenario above or worse.

7 Modelling Lockdowns - Lock-and-Hold vs Lock-and-Reshuffle

In this subsection we focus on the assumptions underlying another modelling choice pertinent to the optimal planner problem – the description of lockdowns in the model. Lockdown is one of the most prevalent non-pharmaceutical interventions (NPIs) used worldwide to control the spread of the disease. They are mandatory or advisory action instituted by the government, imposing social distancing restrictions. In particular, they restrict work and consumption activities, which involve social interactions. We use the afore-going models to offer a brief discussion of the modelling of these lockdown policies.

In what follows, all variables are expressed in stocks, rather than fractions of the population, with the latter stock denoted by POP. The essential disease dynamics as discussed above are governed by

$$\dot{S} = -\beta S \frac{I}{POP} \tag{40}$$

i.e., the product of the pool of the susceptible population S, the relative prevalence of infected people in the population $\frac{I}{POP}$, and the rate at which susceptible people are exposed to the disease β, expressing the intensity of the social interactions and the chance to catch the disease upon an interaction with an infector.

Assume that when the policymaker locks down a share of $(1 - \alpha)$ of the population, the latter are completely isolated from the rest of the population and from each other. Then at a given point in time, no new cases arise in the locked part, and part of the existing cases are resolved. Over time, however, the dynamics depends on the way the lockdown is modelled. We discuss two such ways, which serve to highlight the problematics involved in modelling lockdowns.

7.1 Lock-and-Hold

Consider a lockdown imposed at time t_0 which is general and where we do not know the epidemiological state of each person. Therefore the part of the population that is locked down is selected without knowledge of their state and chosen at random and these same people are held locked down throughout the entire duration of the intervention; we shall use the term "lock-and-hold" for this type of lockdown.

At time t_{0-}, just before lockdown, the following dynamic system holds true:

$$
\begin{aligned}
\dot{S}(t) &= -\beta S(t)\frac{I(t)}{POP} && (41)\\
\dot{E}(t) &= \beta S(t)\frac{I(t)}{POP} - \sigma E(t) && (42)\\
\dot{I}(t) &= \sigma E(t) - \gamma I(t) && (43)\\
\dot{R}(t) &= \gamma I(t) && (44)\\
S(t_{0-}) &= S_0, E(t_{0-}) = E_0, I(t_{0-}) = I_0, && (45)\\
R(t_{0-}) &= R_0, L(t_{0-}) = 0,\\
S+E+I+R+L &= POP
\end{aligned}
$$

where all variables are defined as above and L denotes the pool of people under lockdown.

After lockdown, at time t_{0+}, note that the same set of dynamic equations (41)-(44) holds true. This is so because the number of contacts a susceptible person engages with declines as public spaces, public transportation, and other human gatherings are restricted, and since workplaces are occupied only by the fraction of the population which is not locked, implying an effective transmission rate of $\alpha \cdot \beta$. At the same time, the chance to meet an infector is also computed out of the active population, which is $\alpha \cdot POP$. Therefore, the dynamics of new cases is governed by $\dot{S}(t) = -\alpha \cdot \beta S(t)\frac{I(t)}{\alpha \cdot POP}$ which reduces to equation (41). However, the initial conditions are altered to reflect the lockdown:[12]

$$
\begin{aligned}
S(t_{0+}) &= \alpha S_0, E(t_{0+}) = \alpha E_0, I(t_{0+}) = \alpha I_0, && (46)\\
R(t_{0+}) &= \alpha R_0, L(t_{0+}) = (1-\alpha)POP,\\
S+E+I+R+L &= POP
\end{aligned}
$$

The same dynamics govern the spread of the disease but with different initial conditions. By reducing the size of the interacting population we put the system on a new epidemiological track for the duration of the lockdown, with the same law of motion but starting from different initial conditions.

The implications are dramatic. The effective reproduction number is defined by $\mathcal{R}_e(t) = \mathcal{R}_0 \cdot S(t)$. By slashing the size of the susceptible population, the lockdown can thus control the spread of the disease, and a sufficiently severe lockdown can even drive the effective reproduction number below 1, in which case the disease will be declining as long as the lockdown is in place. Summing up, as long as we are willing to pay the price

[12]For simplicity, we do not separate people within the locked pool $L(t_{0+})$ into the various epidemiological states - the disease in the locked part will just die out gradually.

of forgone output, which is a function of the share of the population that is locked down, this type of lockdown, being intuitive and clear, allows to suppress or control the disease while waiting for cures and vaccines.

7.2 Lock-and-Reshuffle

The quadratic nature of equation (40) above, is reminiscent of the matching process in search models. Some papers in Economics have proposed to use it so as exploit this dynamic property. Note, however, that the implicit assumption here is that we not only lock $(1-\alpha)$ of the population, but that we then release this part, reshuffle with the rest of population, sample randomly again, and lock again. We call this type of lockdown "lock-and-reshuffle." An immediate implication is that an individual's history of lockdowns does not influence the chances of being locked. The re-shuffling should be done continuously, or every period in a discrete time model, in order for the quadratic reduction in cases to occur; one needs to make sure that at each instant, exactly a share α of all susceptibles is active, as well as exactly a share α of all infected. Under these assumptions the essential dynamics of the disease are changed and operate as follows:

$$\begin{aligned} \dot{S}(t) &= -\alpha\beta\alpha S(t)\frac{\alpha I(t)}{\alpha POP} \\ &= -\beta\alpha^2 S(t)\frac{I(t)}{POP} \end{aligned} \tag{47}$$

In this case, for a linear economic cost of lockdown, one gains a quadratic reduction in the spread of the disease. The reason for this result is that the reshuffling and resampling in each period enables the lockdown of more people who are exposed and infectious and therefore puts us in a better position. Though it is a nice feature of the model, such policy is highly unrealistic and impractical. First, we need to assume all workers are interchangeable or that they could be organized in homogenous groups for sampling. Second, the fact that personal history does not influence the chances of getting out of lockdown is unacceptable to people and contradicts basic principles such as fairness, stability, and predictability. People want to know ahead of time whether they will work or not, want to know how long they are expected to stay at home, and want to share the burden of lockdown equally with their peers and not only the expectancy of burden. Furthermore, such mechanisms cannot respect the differentiation between essential and nonessential workers and between workers who can work remotely and those who cannot. We believe that lock and reshuffle is not a plausible policy alternative and that lockdowns should be modelled in more traditional ways. One of the options is the "lock-and-hold" model presented above.

8 Conclusions

The paper has shown how epidemiological dynamics should be modelled and parameterized based on epidemiological analysis. The duration of the infectious stage is crucial for the implied disease dynamics. The widely-used SIR model calibration makes a grave mistake by ignoring the resolved stage, distorting the decisions of the policymaker towards less severe and delayed interventions. Additionally, it makes another, smaller omission by ignoring the latent stage and not considering sub-compartments. Tweaking the initial seed in the baseline SIR model to help the model reach peak infections faster is implausible and is misleading in terms of the predicted burden on the constrained public health system.

We use this model in companion work (see Alon et al (2020)) to explore an optimal planner model optimizing over two dimensions: the degree of lockdown policies and its timing. Both dimensions exploit temporal variation, and rely heavily on the dynamics of the SEIR-Erlang model, including the rate of growth of the disease. The lockdown strategy in this planning problem follows the epidemiological analysis in Karin et al (2020) with the economic planning problem along the lines of equation (39). The emerging optimal policy is quite different from the one proposed thus far in the Economics literature.

References

[1] Acemoglu, Daron, Victor Chernozhukov, Ivan Werning, and Michael D. Whinston, 2020. "A Multi-Risk SIR Model with Optimally Targeted Lockdown" NBER Working Paper No. 27102.

[2] Akbarpour Mohammad, Cody Cook, Aude Marzuoli, Simon Mongey, Abhishek Nagaraj, Matteo Saccarolak, Pietro Tebaldi, and Shoshana Vasserman, 2020. "Socioeconomic Network Heterogeneity and Pandemic Policy Response," BFI, working paper 2020-75.

[3] Alon, Uri , Tanya Baron, Yinon Bar-On, Ofer Cornfeld, Ron Milo, and Eran Yashiv, 2020. "COVID19: Looking for the Exit," working paper, available at

https://www.tau.ac.il/~yashiv/LSE%20June%20paper.pdf

[4] Alvarez, Fernando, David Argente, and Francesco Lippi, 2020. "A Simple Planning Problem for COVID-19 Lockdown," NBER Working Paper No. 26981.

[5] Avery, Christopher, William Bossert, Adam Clark, Glenn Ellison, and Sara Fisher Ellison, 2020. "Policy Implications of Models of the Spread of Coronavirus: Perspectives and Opportunities for Economists," **Covid Economics** 12, 1 May.

[6] Baqaee, David, Emmanuel Farhi, Michael Mina, and James H. Stock, 2020. "Policies for a Second Wave," **Brookings Papers on Economic Activity**, **forthcoming.**

[7] Bar-On, Yinon, Ron Sender, Avi Flamholz, Rob Phillips, and Ron Milo, 2020. "A Quantitative Compendium of COVID-19 Epidemiology," arXiv:2006.01283; available at https://arxiv.org/abs/2006.01283

[8] Champredon, David, Jonathan Dushoff, and David J.D. Earn, 2018. "Equivalence of the Erlang-distributed SEIR Epidemic Model and the Renewal Equation," **SIAM Joural of Applied Math** 78, 6, 3258–3278.

[9] Eichenbaum, Martin S., Sergio Rebelo, and Mathias Trabandt, 2020. "The Macroeconomics of Epidemics," NBER working paper No. 26882.

[10] Ellison, Glenn , 2020. "Implications of Heterogeneous SIR Models for Analyses of COVID-19," NBER Working Paper No. 27373

[11] Farboodi, Maryam, Gregor Jarosch, and Robert Shimer, 2020. "Internal and External Effects of Social Distancing in a Pandemic," NBER Working Paper No. 27059.

[12] Greenstone, Michael and Vishan Nigam, 2020. "Does Social Distancing Matter?" BFI working paper.

[13] Hall, Robert E, Charles I. Jones, and Peter J. Klenow, 2020. "Trading Off Consumption and COVID-19 Deaths,"**Minneapolis Fed Quarterly Review** 42, 1, 2-14.

[14] Imperial College COVID-19 Response Team, 2020. "Report 13: Estimating the number of infections and the impact of non-pharmaceutical interventions on COVID-19 in 11 European countries," available at https://dsprdpub.cc.ic.ac.uk:8443/bitstream/10044/1/77731/10/2020-03-30-COVID19-Report-13.pdf

[15] Johns Hopkins University CSSE, 2020. "2019 Novel Coronavirus COVID-19 (2019-nCoV) Data Repository," Center for Systems Science and Engineering.

[16] Jones, Callum J., Thomas Philippon, Venky Venkateswaran, 2020. "Optimal Mitigation Policies in a Pandemic: Social Distancing and Working from Home," NBER Working Paper No. 26984.

[17] Jones, Charles I. and Jesus Fernandez-Villaverde,2020. "Estimating and Simulating a SIRD Model of COVID-19 for Many Countries, States, and Cities," NBER Working Paper No. 27128.

[18] Kaplan, Greg, Ben Moll, and Gianluca Violante, 2020. "The Great Lockdown: Macroeconomic and Distributional Effects of Covid-19," Manuscript, University of Chicago.

[19] Karin, Omer, Yinon Bar-On, Tomer Milo, Itay Katzir, Avi Mayo, Yael Korem, Avichai Tendler, Boaz Dudovich, Eran Yashiv, Amos J Zehavi, Nadav Davidovitch, Ron Milo and Uri Alon, 2020. "Adaptive cyclic exit strategies from lockdown to suppress COVID-19 and allow economic activity", MedRxiv, available at https://www.medrxiv.org/content/10.1101/2020.04.04.20053579v4.full.pdf

[20] Kermack, William O., and Anderson G. McKendrick, 1927. "A Contribution to the Mathematical Theory of Epidemics," **Proceedings of the Royal Society London**. Ser. A., 115, 700–721.

[21] Krueger, Dirk, Harald Uhlig, and Taojun Xie, 2020. "Macroeconomic Dynamics and Reallocation in an Epidemic," NBER Working Paper No. 27047

[22] Lotka, Alfred J., 1907. "Relation Between Birth Rates and Death Rates," **Science**, 26, 21–22.

[23] Wallinga, Jacco and Marc Lipsitch, 2007. "How Generation Intervals Shape the Relationship between Growth Rates and Reproductive Numbers," **Proceedings of the Royal Society** 274, 599–604

[24] Wearing, Helen J., Pejman Rohani, and Matt J. Keeling, 2005. " Appropriate Models for the Management of Infectious Diseases," **PLoS Medicine** 2, 7, 621-627.

9 Exhibits

Figure 1: The Model

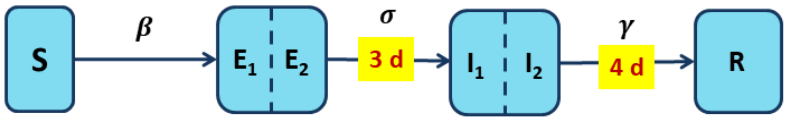

a. The SEIR-Erlang block

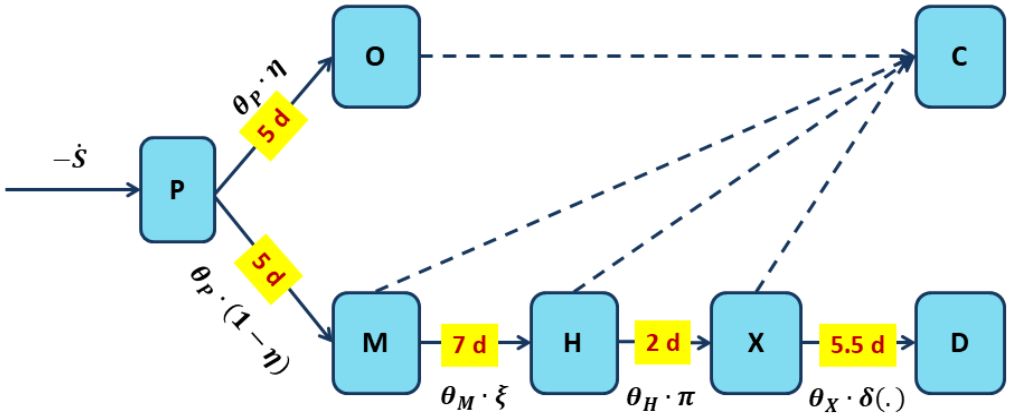

b. The Clinical Block

Table 1 : Epidemiologically-grounded and Clinically-based Parameterization

a. The SEIR-Erlang Block

	Interpretation	Value (source)	Preferred value	Number used
σ	latent period duration	$3-4$ (Compendium)	3	$1/3$
γ	infectious period duration	$4-5$ (Compendium)	4	$1/4$
β	transmission rate			$\gamma \cdot R$

b. The Clinical Block

	Interpretation	Value (source)	Preferred value	Number used
θ_P	incubation period	$5-6$ (Compendium)	5	$1/5$
θ_M	days from symptoms till hospitalization	7 (S1, S2)	7	$1/7$
θ_H	days in hospital till ICU	2 (S3)	2	$1/2$
θ_X	days in ICU before death	5.5 (S3, S4)	5.5	$1/5.5$
η	Prob. to be	$20\%-50\%$ (Compendium)	50%	0.5
	asymptomatic			
ξ	Prob. to get hospitalized when symptomatic	$\frac{\#Hospitalized}{\#Infected} = [2\%-4\%]$ (Compendium)	4%	$\frac{0.04}{1-0.5} = 0.08$
π	Prob. of ICU admission	$10\%-40\%$ (Compendium)	40%	0.4

Notes:

1. Values in third and fourth columns are in days.

2. $\frac{\#Hospitalized}{\#Infected} = \frac{\#Hospitalized}{\#Symptomatic} \cdot \frac{\#Symptomatic}{\#Infected} = \xi \cdot (1-\eta) \implies \xi = \frac{\frac{\#Hospitalized}{\#Infected}}{1-\eta}$

3. Sources:

a. Compendium: Bar-On, Sender, Flamholz, Phillips, and Milo (2020).

b. S1: CDC
https://www.cdc.gov/mmwr/volumes/69/wr/mm6915e3.htm

c. S2: The Lancet
https://www.thelancet.com/action/showPdf?pii=S0140-6736%2820%2930183-5

d. S3: Science
https://science.sciencemag.org/content/early/2020/05/12/science.abc3517/tab-pdf

e. S4: JAMA
https://jamanetwork.com/journals/jama/fullarticle/2765184

Figure 2: Alternative Specifications of the Epidemiological Model

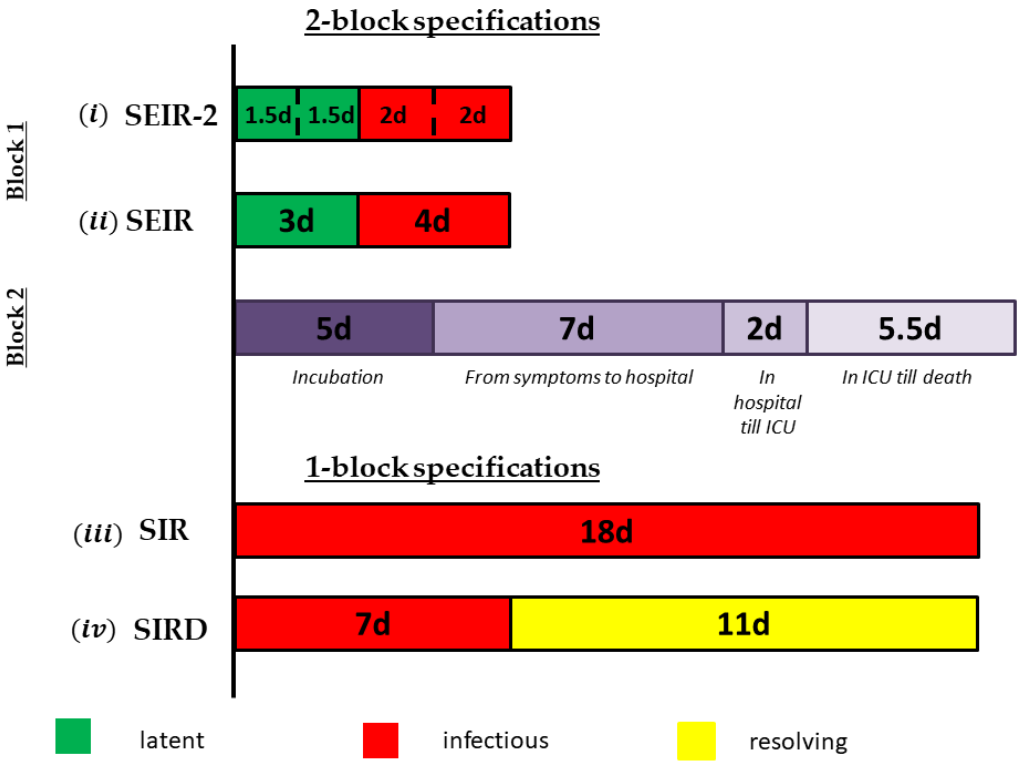

$$
\begin{aligned}
SIR/SIRD &: \mathcal{R} = 1 + \frac{\lambda}{\gamma} \\
SEIR &: \mathcal{R} = \left(1 + \frac{\lambda}{\gamma}\right)\left(1 + \frac{\lambda}{\sigma}\right) \\
SEIR-2 &: \mathcal{R} = \left(1 + \frac{\lambda}{2\gamma}\right)^2 \left(1 + \frac{\lambda}{2\sigma}\right)^2 \frac{1}{1 + \frac{1}{2}\frac{\lambda}{2\gamma}}
\end{aligned}
$$

	2-block specifications		1-block specifications	
	$SEIR$	$SEIR-2$	SIR	$SIRD$
Panel A: Parameterization				
σ	$1/3$	$1/3$	–	–
γ	$1/4$	$1/4$	$1/18$	$1/7$
θ	$n.a^{(a)}$	$n.a^{(a)}$	–	$1/11$
β	$\mathcal{R}_0 \cdot 1/4 = 0.625$	$\mathcal{R}_0 \cdot 1/4 = 0.625$	$\mathcal{R}_0 \cdot 1/18 = 0.139$	$\mathcal{R}_0 \cdot 1/7 = 0.357$
$Scale^{(b)}$	$E + I$	$E_1 + E_2 + I_1 + I_2$	I	I
Panel B: Implied exponential growth rate and doubling time				
$\lambda^{(c)}$	0.17	0.18	0.08	0.21
$t^{(d)}$	4.16	3.91	8.32	3.23
Panel C: Herd immunity and disease scale at peak				
S^*	0.4	0.39	0.4	0.4
$Scale^*$	0.23	0.27	0.23	0.23

Notes:

1. We assume throughout $\mathcal{R}_0 = 2.50$.

2. Notation:

(a) - n.a there is no duration for R in these models and we use the clinical block to provide duration for the clinical progression of the disease.

(b) - scale of the disease - the number of people who are either infectious or are exposed and will become infectious.

(c) - exponential growth rate

(d) - doubling time

3. S^*: Herd immunity - the fraction of susceptibles such that the disease scale reaches its peak. $S^* = 1/\mathcal{R}_0$ for the models with no sub-compartments. In SEIR-2 there is no closed-form expression but $S^* < 1/\mathcal{R}_0$

4. $Scale^*$: Scale of the disease at the peak. For the models with no sub-compartments it is $1 - \frac{1+\ln(\mathcal{R}_0)}{\mathcal{R}_0}$. In SEIR-2 there is no closed-form expression but $Scale^* > 1 - \frac{1+\ln(\mathcal{R}_0)}{\mathcal{R}_0}$.

Figure 3: Disease Dynamics

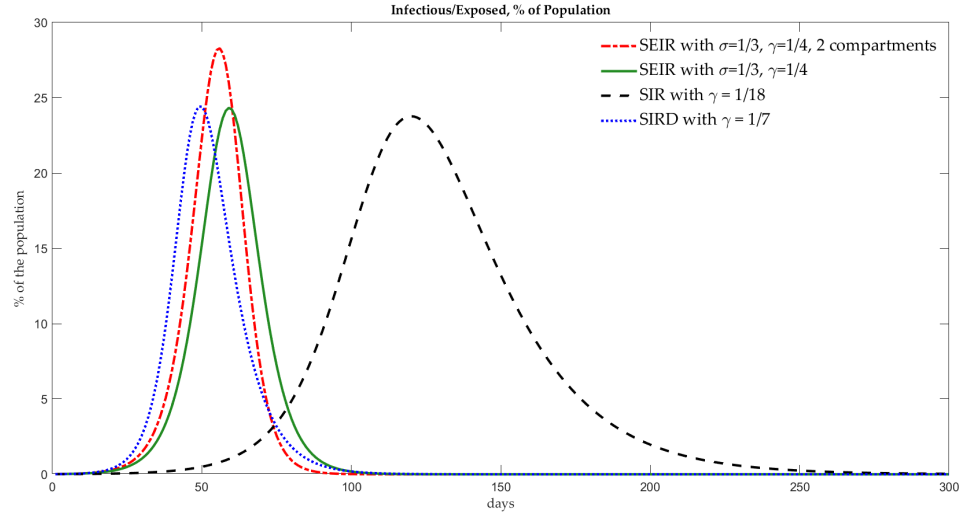

a. Stock of Infectious and Exposed Across the Four Models

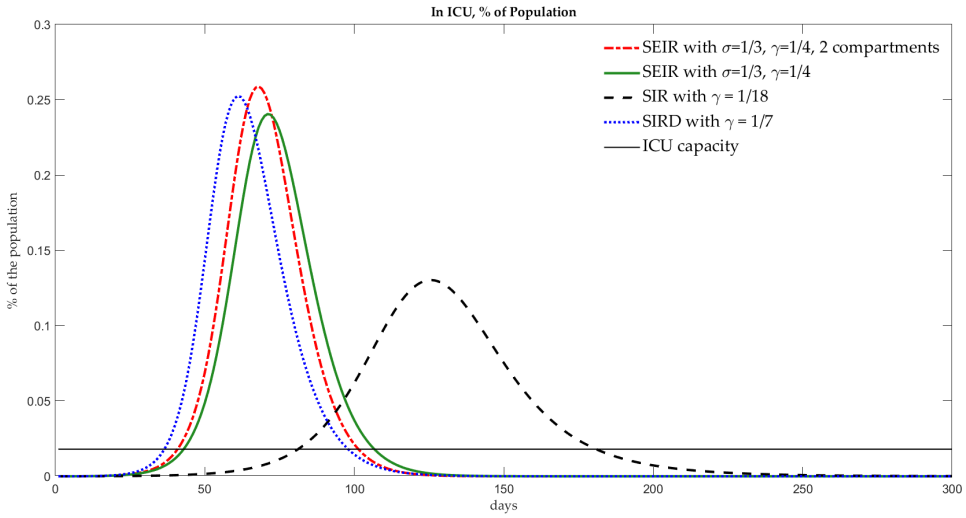

b. X, ICU Utilization Across the Four Models

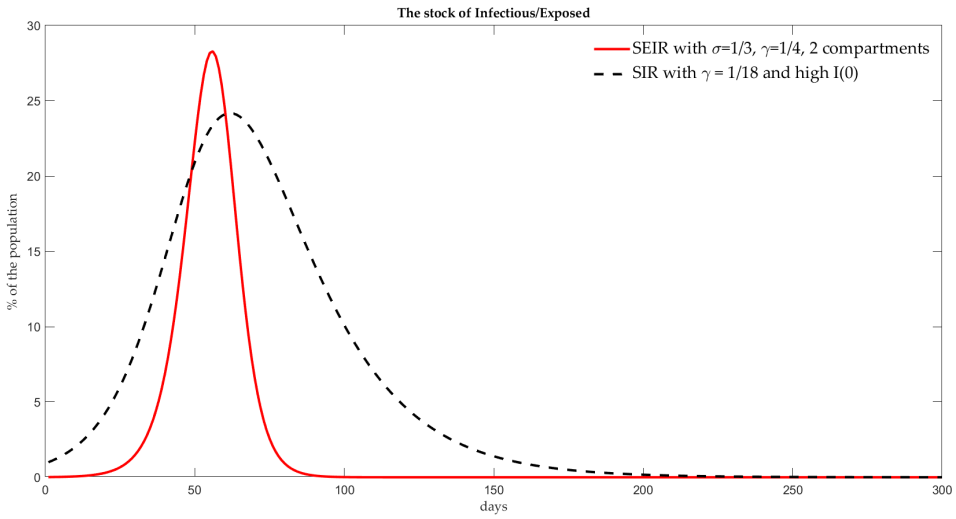

c. Comparing SEIR-2 with seed 10^{-4} and SIR with seed 10^{-2}

Figure 4: Planner Errors

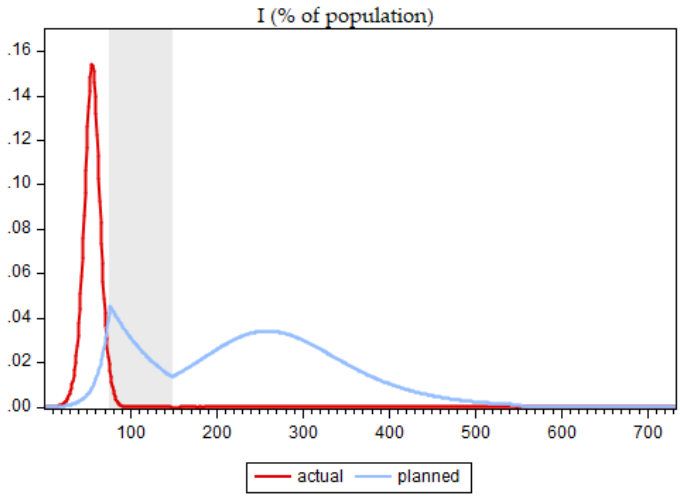

a. Dynamics of I

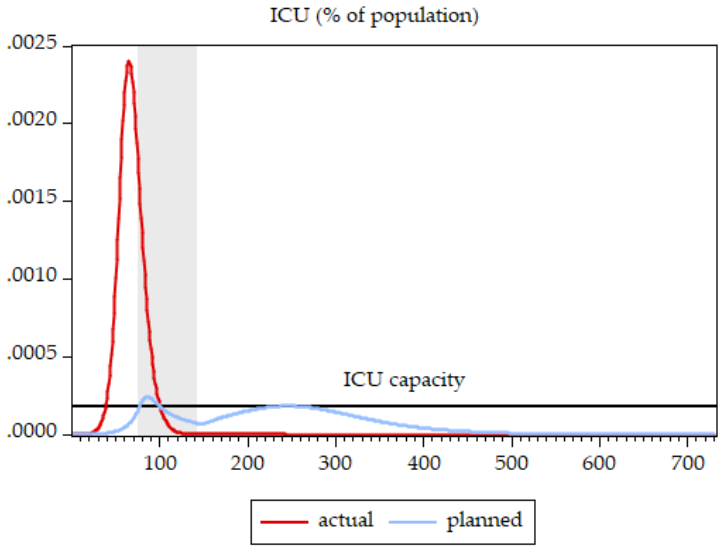

b. Dynamics of X

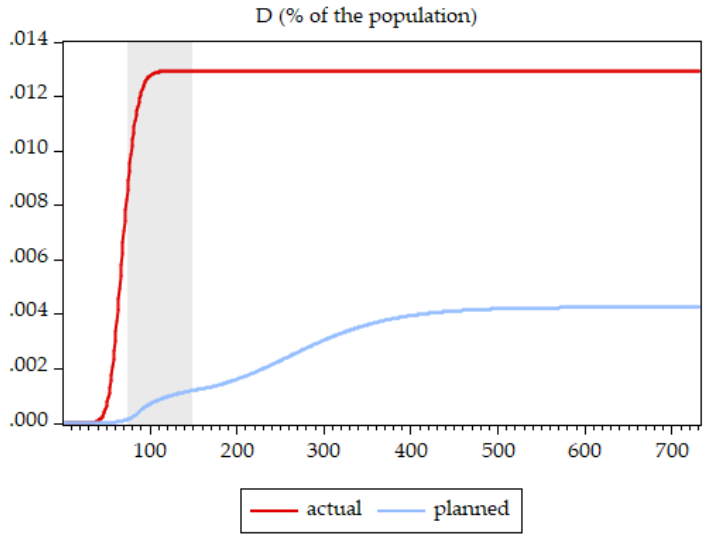

c. Dynamics of D

Note:
Shaded area indicates lockdown period.